Taming Ambident Triazole Anions: Regioselective Ion-Pairing Catalyzes Direct N-Alkylation with Atypical Regioselectivity

Taming Ambident Triazole Anions: Regioselective Ion-Pairing Catalyzes Direct *N*-Alkylation with Atypical Regioselectivity

Harvey J. A. Dale,[†] George R. Hodges,[‡] and Guy C. Lloyd-Jones[†]*

[†] EaStChem, University of Edinburgh, Joseph Black Building, David Brewster Road, Edinburgh, EH9 3FJ, UK

[‡] Syngenta, Jealott's Hill International Research Centre, Bracknell, Berkshire, RG42 6EY, UK

ABSTRACT: Controlling the regioselectivity of ambident nucleophiles towards alkylating agents is a fundamental problem in heterocyclic chemistry. Unsubstituted triazoles are particularly challenging, often requiring inefficient stepwise protection-deprotection strategies and pre-functionalization protocols. Herein we report on the alkylation of archetypal ambident 1,2,4-triazole, 1,2,3-triazole and their anions, analyzed by *in situ* $^{1}H/^{19}F$ NMR, kinetic modelling, diffusion-ordered NMR spectroscopy, X-ray crystallography, highly correlated coupled-cluster computations [CCSD(T)-F12, DF-LCCSD(T)-F12, DLPNO-CCSD(T)] and Marcus theory. The resulting mechanistic insights allow design of an organocatalytic methodology for ambident control in the *direct* *N*-alkylation of unsubstituted triazole anions. Amidinium and guanidinium receptors are shown to act as strongly-coordinating phase-transfer organocatalysts, shuttling triazolate anions into solution. The intimate ion-pairs formed in solution retain the reactivity of liberated triazole anions but, by virtue of highly regioselective ion-pairing, exhibit alkylation selectivities that are completely inverted (1,2,4-triazole) or substantially enhanced (1,2,3-triazole) compared to the parent anions. The methodology allows direct access to 4-alkyl-1,2,4-triazoles (*rr* up to 94:6) and 1-alkyl-1,2,3-triazoles (*rr* up to 99:1) in one step. Regioselective ion-pairing acts in effect as a non-covalent *in situ* protection mechanism, a concept that may have broader application in the control of ambident systems.

INTRODUCTION

Control of regioselectivity in the reaction of ambident nucleophiles with simple electrophiles is of fundamental importance in synthesis, and a perennial problem in heterocyclic chemistry.[1-5] The *N*-alkylation of unsubstituted triazoles – including 1,2,4-triazole, 1,2,3-triazole and benzotriazole – poses a distinctly difficult challenge in this regard.[6-10] Cowden has shown that the *N*-1/*N*-4 selectivity in direct alkylation of 1,2,4-triazole is strikingly insensitive to conventional reaction parameters, Scheme 1.[11] The *N*-1 product is invariably favored over the *N*-4 isomer in an approximately 9:1 ratio, and prior claims of perfect *N*-1 selectivity by use of NaOH/DMF[12] were demonstrated by Cowden to arise from selective extraction of the *N*-4 product during aqueous work-up, not from a change in intrinsic selectivity.[11] In contrast to 1,2,4-triazole, the *N*-alkylation of 1,2,3-triazole affords both regioisomers, with little or no selectivity.[13-16]

Scheme 1. Direct *N*-alkylation of triazoles[a,b]

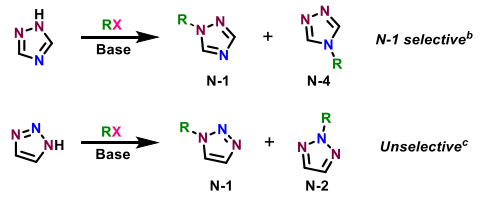

[a]RX = Primary alkylating agent; base is NaOH, DBU etc. [b]Ratio of *N*-1:*N*-4 ≈ 9:1 (F_{N1} ≈ 90 %).[5,11] [c]Ratio of *N*-1:*N*-2 (F_{N1} ≈ 50–65 %).[13,14,17]

The selective *N*-alkylation of 1,2,4-triazole and 1,2,3-triazole currently requires stepwise methodologies, based on classic covalent protection or pre-functionalization protocols that manipulate or otherwise circumvent the intrinsic regioselectivity. For example, *N*-1 acylation of 1,2,4-triazole, reportedly under thermodynamic control, allows selective *N*-4-alkylation then hydrolytic deprotection, Scheme 2 (i).[18] However, the approach suffers from premature hydrolysis and nucleophilic deactivation, necessitating use of very potent oxonium or carboxonium alkylating agents.[18]

Scheme 2. Stepwise strategies for regioselective *N*-alkylation[a]

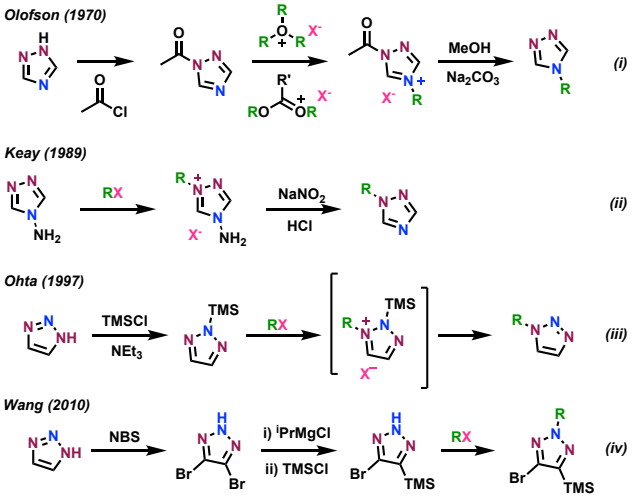

[a]RX = Primary alkylating agent.[13,14,18]

Analogously, 1-alkyl-1,2,4-triazoles can be prepared *via* the alkylation of 4-amino-1,2,4-triazoles and then deamination, Scheme 2 (ii).[19] For 1-alkyl-1,2,3-triazoles, most approaches involves ring-synthesis, e.g. via Cu(I)[20,21] or Ru(II)-catalysed[22,23] azide-alkyne cycloaddition, rather than direct alkyation. Nonetheless, *N*-2 silylation, followed by *N*-1-alkylation and halodesilylation has been reported, Scheme 2 (iii).[13] However, as with acylation (i), the methodology suffers from nucleophilic deactivation and low yields.[13] Regioisomeric 2-alkyl-1,2,3-triazoles can be prepared by *N*-2-selective alkylation of 4-bromo-5-trimethylsilyl-1,2,3-triazole, Scheme 2 (iv);[14] whilst avoiding *N*-protection, the method does however require laborious *C*-4,5 pre-functionalization then de-functionalization.

Herein we report a detailed kinetic, computational and structural investigation into what controls the intrinsic selectivity of alkyla-

tion of 1,2,3- and 1,2,4-triazoles. Based on these mechanistic insights, we then disclose a regioselective, organocatalytic methodology for the *direct N*-alkylation of unsubstituted triazole anions that bypasses the requirement for pre-functionalization (Scheme 2). The new approach exploits an amidinium receptor, which serves as both a *phase-transfer catalyst* and an *in situ, non-covalent protecting group*, shuttling triazole anions into solution to form tightly bound, kinetically competent ion-pairs with high regioselectivity. These ion-pairs retain the reactivity of liberated triazolate anions, but exhibit regioselectivities that are completely inverted (1,2,4-triazole) or substantially enhanced (1,2,3-triazole). Although amidinium and guanidinium cations are used extensively as receptors for organic and inorganic oxyanions – with applications ranging from molecular recognition[24-29] to enantioselective catalysis[30-33] – their deployment as non-covalent protecting agents for ambident nucleophiles, to the best of our knowledge, is unprecedented.

RESULTS AND DISCUSSION

1. Preliminary Studies. We set out with the preliminary objective of rationalizing the intrinsic *N*-1/*N*-4 selectivity (≈ 9:1) in the *N*-alkylation of 1,2,4-triazole,[11] and began by analysis of reactions mediated by the strong organic base MTBD, Scheme 3. For brevity, we denote the selectivity of substitution in terms of the mole fraction (%) of the *N*-1 or *N*-4 alkylated regioisomer, denoted F_{N1} and F_{N4}, respectively. In accordance Cowden,[11] there are only minor deviations in regioselectivity [F_{N1} = 84 – 91 %] across a wide range of primary alkylating agents.

Scheme 3. Regioselectivity (F_{N1}/%) in the *N*-alkylation of 1,2,4-triazole with common alkylating agents[a,b]

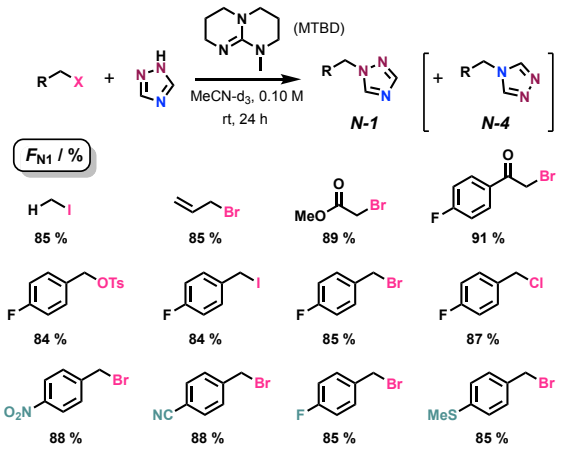

[a]Mole fraction of *N*-1 regioisomer F_{N1} (%) = 100 [N_1]/([N_1]+[N_4]), determined by ^{1}H NMR spectroscopy after full conversion of the alkylating agent. [b]Equimolar quantities of alkylating agent, 1,2,4-triazole and MTBD.

Analysis of the kinetics of *N*-*p*-F-benzylation of 1,2,4-triazole by *in situ* ^{1}H NMR spectroscopy, Figure 1, established that: (i) the rate of substitution is first order with respect to MTBD, with no conversion of *p*-F-BnBr observed in the absence of base; (ii) the *N*-1/*N*-4 partition is *independent* of conversion; and (iii) the selectivity (F_{N1}/%) is insensitive to temperature over the range 20°C – 50°C (Figure S11).

These observations are consistent with a simple anionic mechanism, in which a rapid acid-base pre-equilibrium (K_{PT}) between MTBD and 1,2,4-triazole precedes two competing, *irreversible* substitutions (k_1, k_4, Figure 1). Global fitting of the kinetic profiles of *p*-F-BnBr, *p*-F-BnTrz(*N*-1) and *p*-F-BnTrz(*N*-4) over multiple MTBD loadings (0.20–1.0 equiv.) confirmed the bimolecular nature of the substitutions and afforded values of k_1 = 0.30 M^{-1} s^{-1} ($\Delta^{\ddagger}G_1$(293 K) = 75 kJ mol^{-1}) and k_4 = 0.044 M^{-1} s^{-1} ($\Delta^{\ddagger}G_4$(293 K) = 79 kJ mol^{-1}). On the basis of experimental pK_a values (*vide infra*), MTBD was modelled as a strong base, capable of completely ionizing 1,2,4-triazole (K_{PT} >> 100).

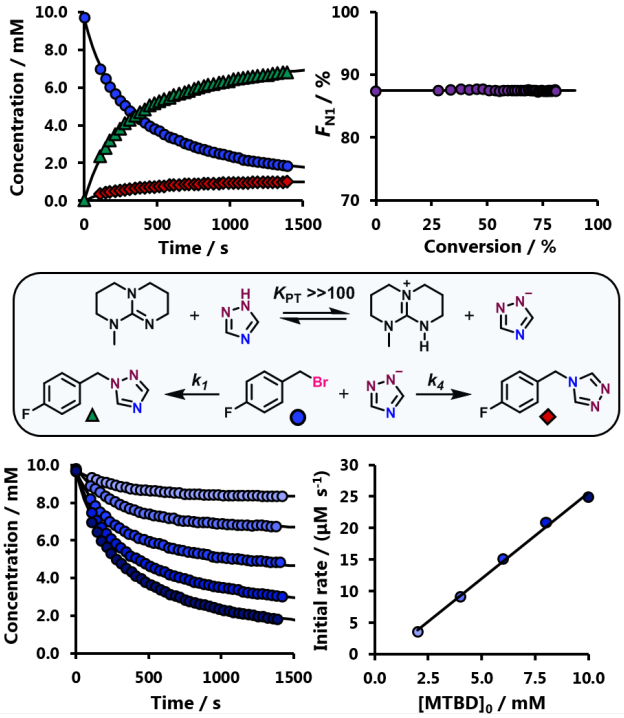

Figure 1. *N*-benzylation of 1,2,4-triazole, analyzed by *in situ* ^{1}H NMR spectroscopy: MeCN-d_3, 20°C: *p*-F-BnBr (10.0 mM), 1,2,4-triazole (10.0 mM), MTBD (2.0 – 10.0 mM); internal standard, 1,3,5-trimethoxybenzene. Solid lines through temporal data are a kinetic model based on anionic mechanism shown, see text for full details.

Highly-correlated CCSD(T)-F12 computations were able to reproduce the free energies of activation ($\Delta^{\ddagger}G_1$, $\Delta^{\ddagger}G_4$) to within chemical accuracy, and the experimental regioselectivity almost quantitatively, by assuming an anionic substitution mechanism under kinetic control, equation 1. Full computational details – including benchmarking of electronic structure theories, solvation models and statistical mechanical approximations – are documented in the Supplementary Information.

$$F_{N_1} = \frac{100\, e^{\frac{(\Delta^{\ddagger}G_4 - \Delta^{\ddagger}G_1)}{RT}}}{1+e^{\frac{(\Delta^{\ddagger}G_4 - \Delta^{\ddagger}G_1)}{RT}}}\ \% \qquad \text{Eq. 1}$$

More efficient, local implementations of coupled-cluster theory (DLPNO-CCSD(T)) were also able to replicate the experimental regioselectivity. Further DLPNO-CCSD(T) computations confirmed that product equilibration, *via* reverse substitution or self-exchange, are kinetically inaccessible under ambient conditions, and moreover that exclusive *N*-1 selectivity would be expected if the reaction were subject to thermodynamic control (Figure S1).

2. Intrinsic Selectivity: Marcus Theory. With greater mechanistic understanding and an accurate computational methodology in hand, we sought to understand the remarkable insensitivity of the *N*-1 selectivity towards common reaction parameters. The combined application of DLPNO-CCSD(T) computations and Marcus theory proved fruitful.[34,35] According to Marcus theory, the free energy of activation $\Delta^{\ddagger}G_i^M$ of an elementary group-transfer reaction can be expressed as a function of the *intrinsic* free energy barrier $\Delta^{\ddagger}G_i^o$ (the arithmetic mean of the free energy barriers for the two corresponding identity reactions, $\Delta^{\ddagger}G_{ii}$ and $\Delta^{\ddagger}G_{BrBr}$, in which there is no thermodynamic contribution to the overall free energy of activation; Figure S2) and the free energy of reaction $\Delta_rG_i^o$, equation 2.

$$\Delta^{\ddagger}G_i^M = \Delta^{\ddagger}G_i^o + \frac{1}{2}\Delta_rG_i^o + \frac{(\Delta_rG_i^o)^2}{16\Delta^{\ddagger}G_i^o} \qquad \text{Eq. 2}$$

In order to elucidate the origin of selectivity, combined KS-DFT and DLPNO-CCSD(T) computations were employed to calculate

$\Delta^{\ddagger}G_i$, $\Delta^{\ddagger}G_i^M$, $\Delta^{\ddagger}G_i^o$ and $\Delta_rG_i^o$ for the *N*-benzylation of 1,2,4-triazolate (Figure 2) at the two competing nucleophilic sites (i = 1,4). Marcus theory ($\Delta^{\ddagger}G_1^M$, $\Delta^{\ddagger}G_4^M$, equation 2) was then able to reproduce the directly-computed free energies of activation ($\Delta^{\ddagger}G_1$, $\Delta^{\ddagger}G_4$) and regioselectivity (F_{N1} = 87 %, F_{N1}^M = 84 %, equation 1) with near quantitative accuracy. The calculations show that the *intrinsic* kinetic barrier for substitution is *higher* at the *N*-1 site than the *N*-4 site ($\Delta^{\ddagger}G_1^o > \Delta^{\ddagger}G_4^o$), and that the observed *N*-1 regioselectivity is driven overwhelmingly by the greater thermodynamic stability of the *N*-1 substituted product ($\Delta_rG_1^o < \Delta_rG_4^o$). In other words, the underlying kinetic preference for *N*-4 substitution is overruled by the thermodynamic preference for *N*-1 substitution: although the reaction proceeds under *kinetic control,* the *thermodynamic stabilization* of the two transition states drives the preferential formation of the *N*-1 regioisomer. The stability differential between the two products is governed primarily by a considerable difference in the intrinsic strengths of the *N*-1 – C_{sp3} and *N*-4 – C_{sp3} bonds ($E_1 - E_4$ = -34 kJ mol^{-1}), which is why the regioselectivity is rendered so insensitive to reaction conditions. These results were confirmed with a range of electronic structure methods (PBE0, DF-LCCSD(T)-F12, DLPNO-CCSD(T)), and DLPNO-CCSD(T) computations elucidated similar trends for a varied selection of other alkylating agents, including AllylBr, $MeOCOCH_2Br$, $PhCOCH_2Br$ (Figure S2).

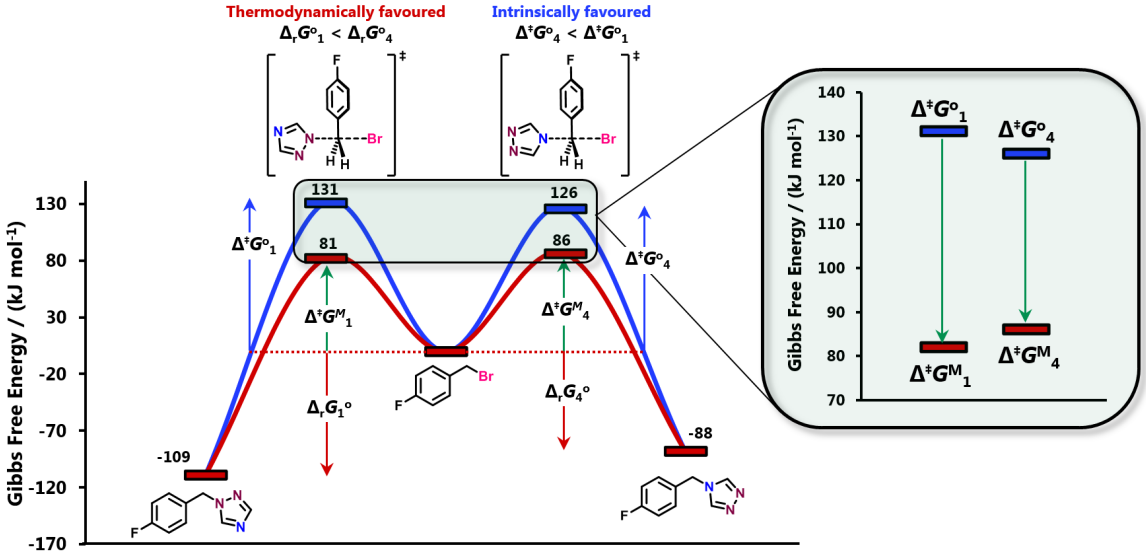

Figure 2. Marcus analysis of the *N*-benzylation of 1,2,4-triazolate with *p*-F-BnBr in MeCN. Free energies of activation and reaction obtained with combined KS-DFT and DLPNO-CCSD(T) computations. Solvation treated implicitly with the IEFPCM (MeCN, UFF) model. See SI.

3. Solvation and Hydrogen-Bonding. The regioselectivity of *N*-benzylation of 1,2,4-triazole under standard reaction conditions (1,2,4-triazole, *p*-F-BnBr, MTBD, 0.10 M) gave end-point regioselectivites of F_{N1} = 76 – 90 % across a diverse range of solvents. With the exception of halogenated solvents ($CHCl_3$, CH_2Cl_2), *N*-1 selectivity was found to be inversely proportional to the ionizing power of the solvent, as quantified by the normalized Dimroth-Reichardt parameter [$E_T(30)$],[36,37] Figure 3.

Combined KS-DFT and CCSD(T)-F12 computations with implicit solvation were able to reproduce this relationship with good accuracy (Figure S3), suggesting that the differential bulk electrostatic stabilization of the two competing transition states broadly governs the overall trend, Figure 3. As expected, however, crude continuum solvation treatments were unable to capture key subtleties of the relationship. This is most apparent in the case of halogenated solvents, which were found to afford atypically low *N*-1 selectivities compared to both computational predictions and non-halogenated solvents of comparable polarity. This inconsistency suggests that the unique role of halogenated solvents as effective hydrogen bond-*donors* but very weak hydrogen bond-*acceptors* either: (i) leads to preferential solvation of the *N*-1 site of 1,2,4-triazolate by weakly regioselective hydrogen-bonding; and/or (ii) promotes *regioselective association* between the conjugate acid $MTBDH^+$ and 1,2,4-triazolate.

The influence of intermolecular complexation was explored by replacing MTBD and 1,2,4-triazole with tetra-*n*-butylammonium 1,2,4-triazolate ($^nBu_4N^+Trz^-$). The difference in regioselectivity $\Delta F_{N1} = F_{N1}(^nBu_4N^+) - F_{N1}(MTBDH^+)$ plotted as a function of the normalized $E_T(30)$ parameter (Figure S3), bears a characteristic signature of regioselective ion-pairing: the difference ΔF_{N1} is greatest for apolar halogenated solvents (CH_2Cl_2, $CHCl_3$) and all but non-existent for highly ionizing protic (MeOH) and aprotic (DMSO) solvents.

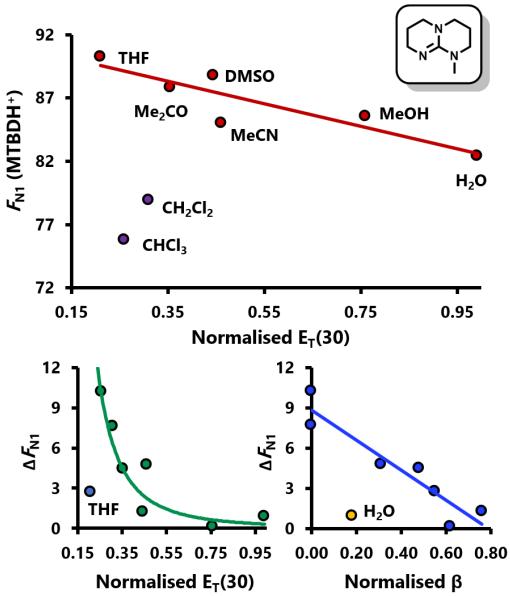

Figure 3. Relationships between regioselectivities (F_{N1}, by ^{1}H NMR) and solvent parameters ($E_T(30)$, β) for the *N*-benzylation of 1,2,4-triazole (0.10 M), *p*-F-BnBr (0.10 M), MTBD (0.10 M) at room temperature. $F_{N1} = [N_1]/([N_1]+[N_4])$.

For halogenated solvents the increases in *N*-1 selectivity upon exchanging MTBDH$^+$ for the weakly-coordinating ^{n}Bu$_4$N$^+$ countercation were particularly significant [$\Delta F_{N1}(CHCl_3)$ = 10 %, $\Delta F_{N1}(CH_2Cl_2)$ = 8 %]. The specific importance of *hydrogen bonding* as the driving force for association between MTBDH$^+$ and 1,2,4-triazolate is highlighted by THF – a solvent less ionizing than both $CHCl_3$ and CH_2Cl_2 – for in this case swapping cations leads to only a minor change in selectivity, contrary to the general trend between F_{N1} and $E_T(30)$. Whereas the *Dimroth-Reichardt* parameter fails to capture this effect, the *Kamlet-Taft* β descriptor – an empirical parameter used to quantify the hydrogen bond basicity of solvents – offers a much better description.[38] According to this descriptor, THF is a highly competent hydrogen bond-acceptor (β_{THF} = 0.55), whilst $CHCl_3$ and CH_2Cl_2 are incapable of serving as hydrogen bond acceptors ($\beta_{CHCl3} = \beta_{CH2Cl2} = 0$) at all. This in turn suggests that THF – unlike $CHCl_3$ and CH_2Cl_2 – would be highly effective in solvating MTBDH$^+$, and therefore in preventing its association with 1,2,4-triazolate.

4. Regioselective Ion-Pairing. The above findings suggested that *regioselective* ion-pairing between a cationic conjugate acid and the 1,2,4-triazolate anion might be exploited to manipulate regioselectivity in *N*-alkylations of 1,2,4-triazole. To investigate this prospect, the impact of a range of strong organic bases[39-41] on the *N*-1 regioselectivity obtained under standard reaction conditions was compared, Chart 1.

Chart 1. Effect of Base on Regioselectivity.[a]

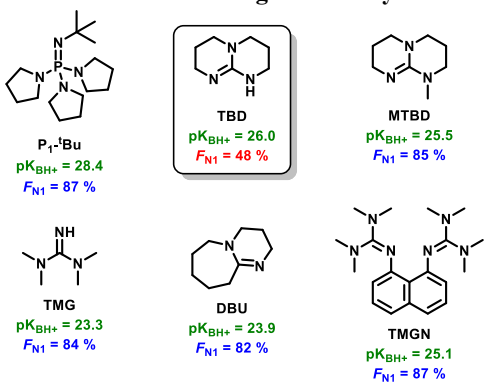

[a]Regioselectivity (F_{N1} / %; end-point) obtained in *N*-benzylation of 1,2,4-triazole with *p*-F-BnBr (MeCN-d_3, 20 °C, 0.10 M) using equimolar organic base. 100 % conversion in < 24h. pK_{BH+} values in MeCN.[39-41]

For the majority of bases, the end-point selectivities were unremarkable (F_{N1} = 82 – 87 %). However, with 1,5,7-triazabicyclo[4.4.0]dec-5-ene (TBD) a major departure from normal selectivity was observed (F_{N1} = 48 %). This outcome suggested that the TBDH$^+$ cation might, uniquely, be able to bind in a *bidentate* manner to 1,2,4-triazolate, with ion-pairing reinforced by a highly directional pair of $^{(+)}$N-H—N$^{(-)}$ hydrogen bonds, Figure 4. In this arrangement, the TBDH$^+$ cation can be considered to serve as a *non-covalent protecting agent* by selectively impeding substitution at the *N*-1 and *N*-2 sites.

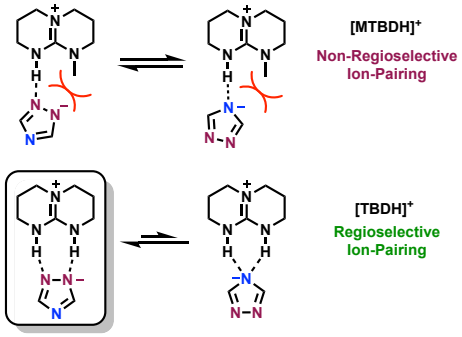

Figure 4. Model for regioselective ion-pairing between TBDH$^+$ and 1,2,4-triazolate, a feature not available to MTBDH$^+$.

5. Kinetics: Conversion and Temperature Dependent Selectivity. For all of the organic bases in Chart 1, *other than TBD*, the regioselectivity (F_{N1} / %) was independent of the extent of 1,2,4-triazolate conversion, consistent with a simple mechanism involving only two directly competing substitution pathways. However, the initial rate of substitution was also found to vary linearly with pK_{BH+}. Because all of the bases will fully ionize 1,2,4-triazole in MeCN (pK_a(MeCN) ~ 8.7, see SI), we attribute this trend to modulation of the reactivity of the 1,2,4-triazolate anion by *non-regioselective* ion pairing with the conjugate acid BH$^+$, and propose that the strength of ion-pairing and reactivity of the 1,2,4-triazolate anion are inversely correlated by virtue of the degree of charge delocalization in BH$^+$.

The kinetics of substitution in the case of TBD, however, are fundamentally different from the other five bases: (i) the *N*-1 selectivity *decreases* significantly with *increasing conversion*; and (ii) the initial rate of substitution is notably suppressed in comparison to MTBD, a base of almost identical strength. Kinetics of this form are suggestive of a dynamic equilibrium between liberated and tightly bound – but nevertheless kinetically competent – 1,2,4-triazolate anions (Trz$^-$), in which the reactivity of the *N*-1/*N*-2 sites of bound triazolate is selectively suppressed by *regioselective complexation* with TBDH$^+$. The rate inhibition in particular suggests that the mode of binding between TBDH$^+$ and 1,2,4-triazolate is distinct from the other conjugate acids, with non-regioselective ion-pairing reinforced by significant hydrogen bonding. Under such a regime the decrease in *N-1* selectivity over the course of the reaction suggests that the ratio of bound triazolate to free triazolate increases with conversion; indeed, it can be proved analytically that this *must* be so in the case of a rapid complexation equilibrium (see proof S1).

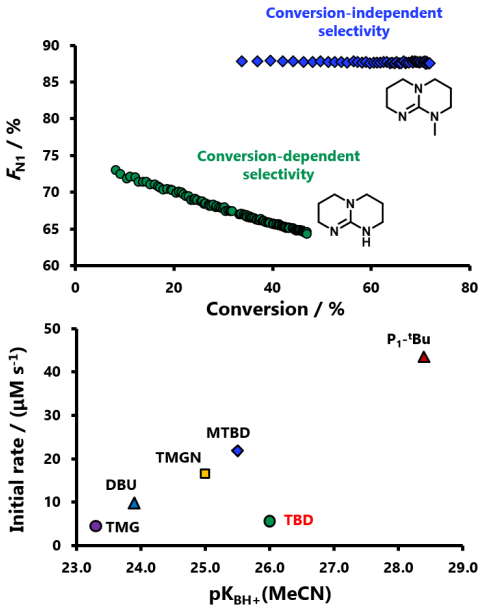

Figure 5. Selectivity-conversion profiles for the N-benzylation of 1,2,4-triazole (10.0 mM) with *p*-F-BnBr (10.0 mM) and TBD (10.0 mM) or MTBD (10.0 mM) in MeCN-d_3 (20°C). Initial rate–pK_{BH+} plot obtained under the same conditions for all bases. Selectivity-conversion profiles of TMG, DBU, TMGN and P$_1$-^{t}Bu are in Figure S5.

Reactions mediated by TBD were also uncharacteristically sensitive towards temperature, with lower temperatures leading to systematically higher *N*-4 selectivities [F_{N1}(-20°C) = 32 % → F_{N1}(40°C) = 55 %]. Such thermal sensitivity may be attributed to the *exothermicity* of the association of TBDH$^+$ and triazolate, for under a non-associative regime the regioselectivity ought not to change by more than 5% over the same temperature range ([3], T_α = 253 K, T_β = 313 K, $\Delta^\ddagger G_4 - \Delta^\ddagger G_1$ = 4.7 kJ mol^{-1}). Moreover, in the

absence of regioselective ion-pairing, lower temperatures should promote the formation of the kinetically favoured *N*-1 regioisomer, contrary to experimental findings.

$$\frac{F_1(T_\alpha)}{F_1(T_\beta)} = \frac{e^{\frac{(\Delta^\ddagger G_4 - \Delta^\ddagger G_1)}{RT\alpha}}\left(1+e^{\frac{(\Delta^\ddagger G_4 - \Delta^\ddagger G_1)}{RT\beta}}\right)}{e^{\frac{(\Delta^\ddagger G_4 - \Delta^\ddagger G_1)}{RT\beta}}\left(1+e^{\frac{(\Delta^\ddagger G_4 - \Delta^\ddagger G_1)}{RT\alpha}}\right)} \qquad \text{Eq. 3}$$

6. [TBDH]$^+$ H-bonding: Impact of Solvent and Counter-ion. In contrast to MTBD, where the *N*-1 / *N*-4 selectivity varies little with solvent, TBD was found to be highly sensitive, Scheme 4. Polar aprotic or protic solvents give conventional selectivity [F_{N1}(DMSO) = 85 %, F_{N1}(MeOH) = 83 %]; apolar solvents lead to enhanced *N*-4 selectivity [F_{N1}(CH_2Cl_2) = 38 %, F_{N1}(THF) = 38 %].

Scheme 4. Solvent effects for the *N*-benzylation of 1,2,4-triazole with MTBD versus TBD[a,b,c]

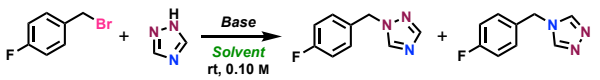

F_{N1} / %	DMSO	MeOH	MeCN	Me_2CO	THF	CH_2Cl_2
MTBD	89	86	85	88	90	79
TBD	85	83	48	49	38	38

[a]F_{N1} = [N_1]/([N_1]+[N_4]). [b]Ratio of regioisomers determined by ^{1}H NMR spectroscopy after full conversion of *p*-F-BnBr. [c]Equimolar quantities of 1,2,4-triazole, p-F-BnBr and MTBD/TBD.

The effect of exogenous guanidium salts (TBDH$^+$X$^-$, 1 equiv., Figure 6) on the standard reaction proved particularly instructive. Strongly-coordinating counteranions (X$^-$ = Cl$^-$) imparted no effect on the end-point regioselectivity [F_{N1}(Cl$^-$) = 48 %], whereas weakly-coordinating anions (X$^-$ = I$^-$, PF_6^-, BPh_4^-) facilitated significant enhancements in *N*-4 selectivity [F_{N1}(I$^-$) = 32 %, F_{N1}(PF_6^-) = 31 %, F_{N1}(BPh_4^-) = 31 %]. Intermediate regioselectivities were attained with TBDH$^+$Br$^-$ [F_{N1}(Br$^-$) = 39 %]. Reliable comparisons with TBDH$^+$AcO$^-$ were precluded by competing *O*-benzylation.

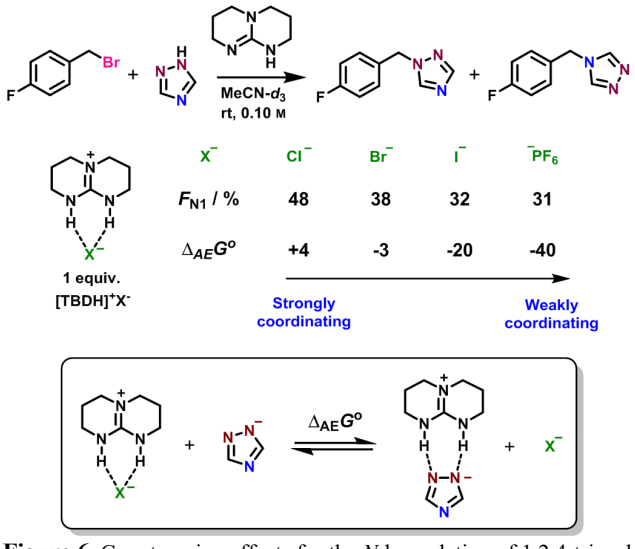

Figure 6. Counteranion effects for the *N*-benzylation of 1,2,4-triazole with TBD and TBDH$^+$X$^-$ additives. F_{N1} = [N_1]/([N_1]+[N_4]). Ratio of regioisomers determined by ^{1}H NMR spectroscopy after full conversion of *p*-F-BnBr. Equimolar quantities of 1,2,4-triazole, *p*-F-BnBr, TBD and TBDH$^+$X$^-$. Theoretical free energies of anion exchange ($\Delta_{AE}G°$) computed with a combined KS-DFT/DLPNO-CCSD(T) methodology.

DLPNO-CCSD(T) computations revealed that the displacement of X$^-$ from the TBDH$^+$ binding site by 1,2,4-triazolate is strongly endergonic for X$^-$ = Cl$^-$, mildly endergonic for X$^-$ = Br$^-$ and highly exergonic for X$^-$ = I$^-$ and PF_6^-, reflecting the respective effects of the TBDH$^+$X$^-$ salts on regioselectivity (Figure 6). Thus, when X$^-$ is weakly-coordinating, addition of TBDH$^+$X$^-$ to the reaction creates an additional reservoir of cationic receptor TBDH$^+$, thereby promoting triazolate binding by mass action; when X$^-$ is strongly coordinating the excess TBDH$^+$ remains inaccessible to the triazolate. In a further manifestation of this effect, exchanging *p*-F-BnBr [F_{N1}(*p*-F-BnBr) = 48 %] for *p*-F-BnCl lead to a notable deterioration in *N*-4 selectivity [F_{N1}(*p*-F-BnCl) = 60 %], whilst *p*-F-BnI conversely lead to an improvement [F_{N1}(*p*-F-BnI) = 40 %] (Figure S13).

7. Experimental Characterization of the TBDH-triazolate Ion-Pair. Crystallization of TBDH$^+$Trz$^-$ from CH_2Cl_2/pentanes furnished monoclinic crystals (*C*2/*c*) suitable for X-ray diffraction. In agreement with our hypothesis, the crystal structure (see later) shows the TBDH$^+$ cation serving as a *bidentate* hydrogen-bond donor to the *N*-1/*N*-2 sites of the triazolate anion, with **N**H – **N** distances of 2.84 Å.

To provide solution-phase evidence for ion-pairing we used diffusion-ordered ^{1}H NMR spectroscopy (DOSY) to characterize separate 0.1 M solutions of i) ^{n}Bu$_4$N$^+$Trz$^-$, ii) TBDH$^+$$PF_6^-$, and iii) ^{n}Bu$_4N^+Trz^-$ + TBDH$^+$$PF_6^-$ in MeCN-d_3 containing 1,3,5-trimethoxybenzene and tetramethylsilane (TMS) as internal diffusion standards (Figure S6). The diffusion constant of ^{n}Bu$_4$N$^+$ was identical between samples i and iii, as expected of a weakly-coordinating cation. However, compared to i, and ii, the diffusion constants of TBDH$^+$ and 1,2,4-triazolate in sample iii decreased significantly and converged, consistent with the formation of a non-covalent association complex between TBDH$^+$ and Trz$^-$.

Under the approximations of the Stokes-Einstein equation – and assuming *strong* association – a value of $V_{Complex}/V_{TBDH+} \approx 1.23$ was calculated for the ratio of the molecular volumes in MeCN (Figure S6). KS-DFT computations of TBDH$^+$Trz$^-$ (see Section 8) suggest that $V_{TBDH+Trz}/V_{TBDH+} \approx 1.24$, strongly supporting the assignment of the solution-phase ion-pair complex as a monomer. Kinetic modelling data (*vide infra*) suggest that the assumption of strong association is a valid one (Figure S6).

8. Computational Characterization of the TBDH-triazolate Ion-Pair. Using combined KS-DFT and highly correlated DLPNO-CCSD(T) computations we explored possible structures of the TBDH$^+$Trz$^-$ complex, the thermodynamic feasibility of complexation, the underlying constitution of the interaction (ion-pairing *vs.* hydrogen-bonding *vs.* dispersion) and the kinetic competency of TBDH$^+$Trz$^-$ towards *N*-benzylation. Gibbs free energies were computed using standard statistical mechanical approximations (see SI for details).

Three distinct structures of the complex were obtained following KS-DFT optimizations, Figure 7: (i) an exclusively hydrogen-bonded complex between neutral 1,2,4-triazole and TBD, with no charge separation; (ii) a non-specific ion-paired complex, in which the triazolate anion adopts a facial orientation with respect to the HN-C-NH plane of TBDH$^+$; and (iii) an ion-paired complex reinforced by a pair of directional NH—N hydrogen bonds, in which the HN-C-NH core of TBDH$^+$ and the 1,2,4-triazolate anion exist in a coplanar configuration. DLPNO-CCSD(T) computations predict that the third of these structures is considerably lower in free energy than the other alternatives, including unbound states, with a solution-phase binding energy of $\Delta_{Bind}G_{Trz}$(TBD) = -18 kJ mol^{-1} relative to the free ions. Computations also suggest that TBDH$^+$ will be *selective* toward 1,2,4-triazolate anions in the presence of bromide, with a difference in binding free energy of $\Delta\Delta_{Bind}G$(TBD) = 4 kJ mol^{-1} (equation 4, Figure S7).

$$\Delta\Delta_{\mathrm{Bind}}G(\mathrm{TBD}) = \Delta_{\mathrm{Bind}}G_{\mathrm{Br}}(\mathrm{TBD}) - \Delta_{\mathrm{Bind}}G_{\mathrm{Trz}}(\mathrm{TBD}) \qquad \text{Eq. 4}$$

$$\Delta\Delta^{\ddagger}G'(\mathrm{TBD}) = \Delta^{\ddagger}G_4'(\mathrm{TBD}) - \Delta^{\ddagger}G_1'(\mathrm{TBD}) \qquad \text{Eq. 5}$$

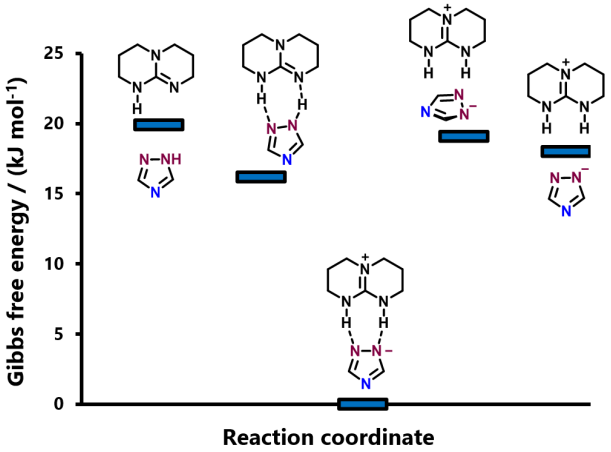

Figure 7. Computational characterisation of the TBDH$^+$Trz$^-$ ion-pair. Gibbs free energies were obtained from combined KS-DFT and DLPNO-CCSD(T) computations, using the ideal-gas rigid-rotor harmonic oscillator (IGRRHO) approximation.

Transition states for the benzylation of *N*-1 and *N*-4 with the 1,2,4-triazolate anion docked in the binding site of TBDH$^+$ (*p*-F-BnBr, Figure 8) gave computed free energies of activation for the two competing pathways [$\Delta^{\ddagger}G_1$'(TBD), $\Delta^{\ddagger}G_4$'(TBD), Figure 8] in which complexation leads to an *inversion* of regioselectivity: once bound, *N*-4 substitution of triazolate is rendered more favourable than *N*-1 [$\Delta\Delta^{\ddagger}G'$(TBD) = -7.1 kJ mol^{-1}].

Indeed, the computed barrier to *N*-1 substitution is significantly elevated [$\Delta^{\ddagger}G'_1$(TBD) > $\Delta^{\ddagger}G_1$; $\Delta\Delta^{\ddagger}G'_1$(TBD) = 6.1 kJ mol^{-1}] by TBDH$^+$ binding, whereas the barrier to *N*-4 substitution appears to be reduced [$\Delta^{\ddagger}G'_4$(TBD) < $\Delta^{\ddagger}G_4$; $\Delta\Delta^{\ddagger}G'_1$(TBD) = -6.4 kJ mol^{-1}].

$$\Delta\Delta^{\ddagger}G'_1(\mathrm{TBD}) = \Delta^{\ddagger}G'_1(\mathrm{TBD}) - \Delta^{\ddagger}G_1 \qquad \text{Eq. 6}$$

$$\Delta\Delta^{\ddagger}G'_4(\mathrm{TBD}) = \Delta^{\ddagger}G'_4(\mathrm{TBD}) - \Delta^{\ddagger}G_4 \qquad \text{Eq. 7}$$

Whilst the transition state for *N*-4 substitution remains fundamentally unaffected by complexation with TBDH$^+$, the ion-pair must undergo substantial structural rearrangements to expose the *N*-1 site of the 1,2,4-triazolate anion. To interact with the incoming electrophile, the anion must twist out of the HN-C-NH plane of TBDH$^+$, forcing both of the guanidinium protons to form hydrogen bonds with the *N*-2 site in a distorted, clamp-like binding mode. Moreover, in the *N*-1 transition state the bromide anion remains partially encapsulated by the cation, leading to: (i) a significant reduction in the solvation energy of the *N*-1 transition state relative to the *N*-4 TS; and (ii) secondary ionic interactions between Br$^-$ and TBDH$^+$. Overall, the combined influences of weakened solvation and hydrogen bond distortion lead to the relative destabilization of the *N*-1 TS.

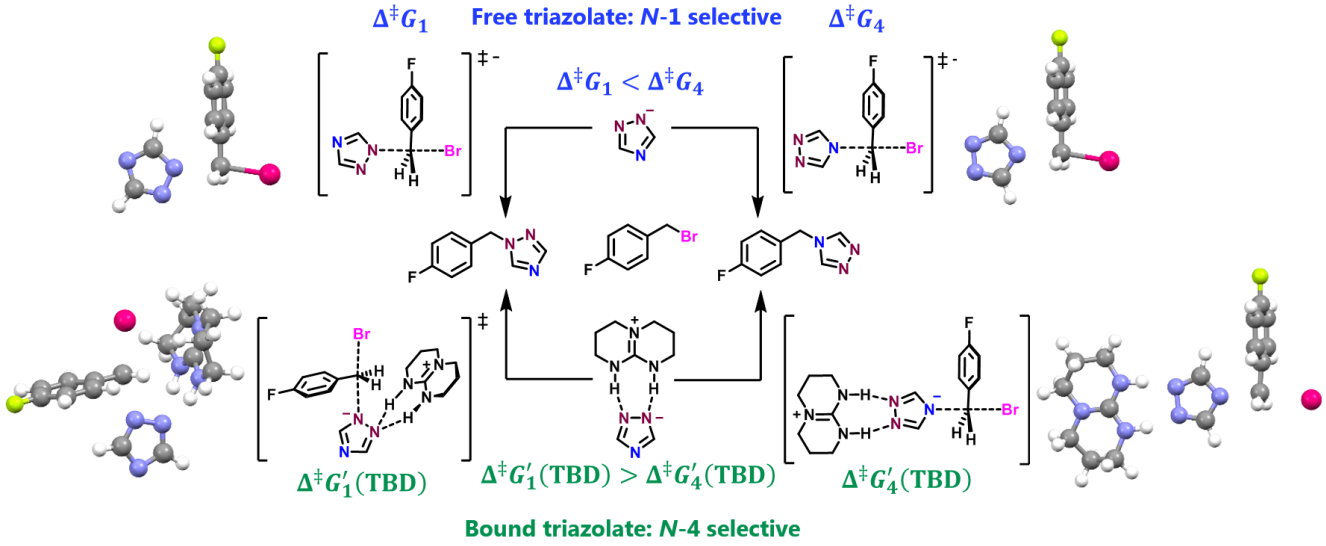

Figure 8. Computed transition states for the *N*-benzylation of the 1,2,4-triazolate anion (free and bound). $\Delta^{\ddagger}G_1$ = 81 kJ mol^{-1} and $\Delta^{\ddagger}G_4$ = 86 kJ mol^{-1} denote free energies of activation for the *N*-benzylation of liberated 1,2,4-triazolate anions; $\Delta^{\ddagger}G'_1$ = 87 kJ mol^{-1} and $\Delta^{\ddagger}G'_4$ = 80 kJ mol^{-1} denote the free energy barriers for the bound anion. Free energies computed using a combined KS-DFT/DLPNO-CCSD(T) methodology (see SI) and the ideal-gas rigid-rotor harmonic-oscillator (IGRRHO).

9. Kinetic Characterization. To tension the computed intrinsic selectivity [$\Delta\Delta^{\ddagger}G$(TBD)] and binding free energy [$\Delta_{\mathrm{Bind}}G_{\mathrm{Trz}}$°(TBD)] of the TBDH$^+Trz^-$ ion-pair with experiment, we developed a kinetic model for the *N*-benzylation of 1,2,4-triazolate in the presence of TBD (Figure 9). The most general version of the model consists of: (i) an acid-base equilibrium between TBD and 1,2,4-triazole (K_{PT}); (ii) a rapid binding equilibrium between TBDH$^+$ and 1,2,4-triazolate (K_{Trz}); (iii) four substitution pathways, including two for unbound triazolate (k_1, k_4) and two involving tightly bound triazolate (k'_1, k'_4); and (iv) a deleterious binding equilibrium between TBDH$^+$ and Br$^-$ (K_{Br}). The two rate coefficients k_1 = 300 mM^{-1} s^{-1} and k_4 = 44 mM^{-1} s^{-1} were obtained using MTBD as a base (*vide supra*).

According to this model the instantaneous *N*-1 selectivity (S_1) is afforded by the ratio given in Equation 8, and it can be proved analytically that S_1 is always a decreasing function in [TBDH$^+$Trz$^-$]/[Trz$^-$] (see Proof S2) when Equation 9 holds. Because [TBDH$^+$Trz$^-$]/[Trz$^-$] must increase with conversion (Proof S1), S_1 decreases over the course of the reaction, Figure 5.

$$S_1 = \frac{k_1 + k'_1[\mathrm{TBDH^+Trz^-}]/[\mathrm{Trz^-}]}{k_1 + k_4 + (k'_1 + k'_4)[\mathrm{TBDH^+Trz^-}]/[\mathrm{Trz^-}]} \qquad \text{Eq. 8}$$

$$\frac{k_1}{k_4} > \frac{k'_1}{k'_4} \qquad \text{Eq. 9}$$

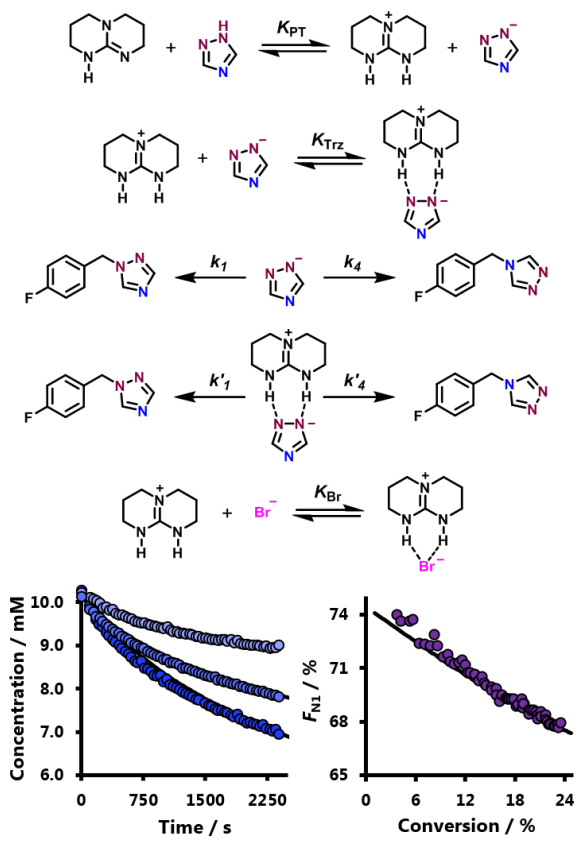

Figure 9. Formal kinetic model for the *N*-benzylation of 1,2,4-triazole with *p*-F-BnBr in the presence of TBD. Binding equilibria are assumed to be rapid. Rate coefficients k_1 = 300 mM^{-1} s^{-1} and k_4 = 44 mM^{-1} s^{-1} obtained from kinetic modelling with MTBD *(vide supra)*. Kinetic profiles of *p*-F-BnBr obtained by *in situ* ^{1}H NMR spectroscopy in MeCN-d_3, 20°C: *p*-F-BnBr (10.0 mM), 1,2,4-triazole (10.0 mM), TBD (1.5, 3.0, 5.0 mM); example selectivity-conversion profile shown for [TBD]$_0$ = 3.0 mM. Model shown as black lines. F_{N1} = [N$_1$]/([N$_1$]+[N$_4$]).

Datasets from in situ ^{1}H NMR analysis of the *N*-benzylation reaction in MeCN-d_3, under a wide range of initial concentrations of TBD were subjected to a global kinetic analysis (Figure S7). The fitted rate coefficients (k'_1, k'_4) and binding constants (K_{Trz}, K_{Br}) are summarized in Table 1 (Model 1). In accordance with experimental pK_a values [pK_a(Trz, MeCN) ~ 8.7; pK_{BH+}(TBD, MeCN) = 26.0] it was assumed that 1,2,4-triazole is fully ionized by TBD (K_{PT} >> 100); however, the results of kinetic fitting were almost completely unaffected for all values of K_{PT} > 0.1. We also tested a simplified model in which the binding equilibrium between TBDH$^+$ and Br$^-$ was neglected completely (Model 2).

There is good agreement between the kinetic model (Table 1) and DLPNO-CCSD(T) computations, with both approaches capturing the same key conclusions: (i) the inversion of selectivity upon binding is driven in part by a substantial elevation in the barrier to substitution at the *N*-1 site [$\Delta\Delta^{\ddagger}G'_1$(TBD) > $\Delta\Delta^{\ddagger}G'_4$(TBD)]; and (ii) the TBDH$^+$ cation strongly and selectively binds triazolate in preference to extruded bromide [$\Delta\Delta_{Bind}G$(TBD) =10 kJ mol^{-1}, Model 1]. Indeed, the extent of agreement is remarkable given the significant challenges inherent in accurately modelling the non-covalent interactions between, and solvation of, ionic fragments. The most significant discrepancy is the change in *N*-4 reactivity upon TBDH$^+$ complexation, where computations suggest that binding between TBDH$^+$ and 1,2,4-triazolate should reduce the barrier to *N*-4 substitution ($\Delta\Delta^{\ddagger}G'_4$(TBD) < 0), but both kinetic models suggest that it increases ($\Delta\Delta^{\ddagger}G'_4$(TBD) > 0), presumably as a consequence of charge-transfer. We ascribe this inconsistency to computational deficiencies in the treatment of vibrational entropies; application of Grimme's quasi rigid-rotor harmonic-oscillator (qRRHO) approximation leads to significantly improved agreement between experimental and computed selectivities ($\Delta\Delta^{\ddagger}G$, $\Delta\Delta^{\ddagger}G'$, $\Delta\Delta^{\ddagger}G'_1$ and $\Delta\Delta^{\ddagger}G'_4$).

Table 1. Kinetic parameters and binding energies for the N-benzylation of 1,2,4-triazole with *p*-F-BnBr and TBD[a,b,c,d]

TBD	Model 1	Model 2	IGRRHO	qRRHO
$\Delta\Delta^{\ddagger}G$	4.7	4.7	5.4	4.8
$\Delta\Delta^{\ddagger}G'$	3.2	1.8	7.1	5.8
$\Delta\Delta^{\ddagger}G'_1$	10.8	9.5	6.1	8.4
$\Delta\Delta^{\ddagger}G'_4$	3.0	3.0	-6.4	-2.2
$\Delta_{Bind}G_{Trz}$	-22	-22	-22	-18
$\Delta_{Bind}G_{Br}$	-13	-	-18	-15
$\Delta\Delta_{Bind}G$	10	-	4	3

[a]All free energies quoted in kJ mol^{-1}. Experimental free energies of activation obtained from classical transition state theory, using the Eyring-Polanyi equation and fitted rate coefficients from kinetic modelling. [c]Experimental rate coefficients obtained by *in situ* ^{1}H NMR spectroscopy. [d]Computed parameters obtained with a combined KS-DFT/DLPNO-CCSD(T) methodology and the IGRRHO or Grimme's qRRHO approximations (ω_c = 100 cm^{-1}).

10. Optimization of Ambident Control. With mechanistic insight to the ambident reactivity of the 1,2,4-triazolate anion, we turned our attention to application of this in synthesis, and in particular optimizing the selectivity of alkylation, and the stoichiometry of TBD required. DLPNO-CCSD(T) computations suggested highly exergonic TBDH$^+$ / Trz$^-$ binding in apolar solvents. The low selectivity in such solvents (Scheme 4) suggested that it is residual reactivity of the *N*-1 site in the ion-pair, rather than insufficient binding *per se*, that required attenuation. With this in mind, we studied the conjugate acid of PMD, a commercially available amidine (Figure 10) in which greater charge localization in the PMDH$^+$ cation, relative to TBDH$^+$, should increase its affinity for triazolate.

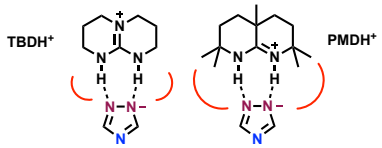

	TBDH⁺Trz⁻	PMDH⁺Trz⁻	DLPNO-CCSD(T):
$\Delta_{Bind}G_{Trz}$	-22	-36	Increased binding affinity
$\Delta\Delta_{Bind}G$	4	8	Increased binding selectivity
$\Delta^{\ddagger}G'_1$	87	94	Increased N-1 protection
$\Delta^{\ddagger}G'_4$	80	80	Similar N-4 protection
$\Delta\Delta^{\ddagger}G'$	7	14	Higher kinetic selectivity

Figure 10. Computational comparison of the TBDH$^+$Trz$^-$ and PMDH$^+$Trz$^-$ ion-pairs. Free energies obtained from combined KS-DFT/DLPNO-CCSD(T) computations, using the ideal-gas rigid-rotor harmonic-oscillator (IGRRHO) approximation.

Moreover, the four methyl substituents flanking the amidinium protons in PMDH$^+$ should augment the protection of the *N*-1/*N*-2 sites. Indeed, DLPNO-CCSD(T) computations suggested that both the binding free energy of PMDH$^+$ and Trz$^-$ [$\Delta_{Bind}G$(PMD)] and the kinetic selectivity of the PMDH$^+$Trz$^-$ ion-pair [$\Delta\Delta^{\ddagger}G'$(PMD)] would exceed those of TBD (Figure 10). A Local Energy Decomposition (LED) analysis (Figure S8) revealed that the increased binding energy of PMDH$^+$ and 1,2,4-triazolate can be decomposed into two major contributions: (i) enhanced London dispersion interactions between the two ionic fragments; and (ii) a reduction in the geometric and electronic distortion energies of the cation. Computations additionally suggested that PMDH$^+$ ought to be more *selective* for 1,2,4-triazolate than TBDH$^+$ in the presence of competing bromide anions [$\Delta\Delta_{Bind}G$(PMD) > $\Delta\Delta_{Bind}G$(TBD)].

These predictions were confirmed experimentally for the *N*-benzylation of 1,2,4-triazole (*p*-F-BnBr, 0.10 M), with *N*-4 selectivity

increasing significantly upon exchanging TBD [$F_{N1}(CH_2Cl_2)$ = 38 %] for PMD [$F_{N1}(CH_2Cl_2)$ = 6 %]. As for TBD, the regioselectivity remained characteristically sensitive to the ionizing strength of the solvent and the charge density of the leaving group (Figures S12-13). *In situ* reaction monitoring by ^{1}H NMR spectroscopy (Figure 11) confirmed that PMD shows the same kinetic behavior as TBD, with *N*-4 selectivity increasing at higher conversions and lower temperatures; as for TBD, the rate of substitution was found to be cleanly first-order in PMD (Figure S9).

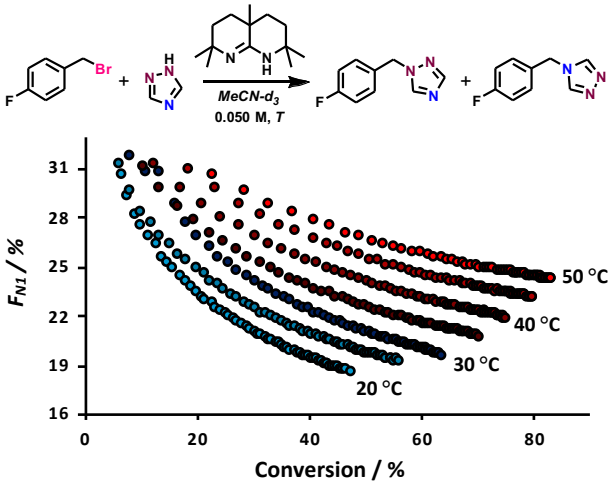

Figure 11. Selectivity-conversion profile for the *N*-benzylation of 1,2,4-triazole (50.0 mM) with *p*-F-BnBr (50.0 mM) and PMD (50.0 mM) over a range of temperatures (20°C – 50°C, 5°C increments). [a]F_{N1} = $[N_1]/([N_1]+[N_4])$.

Table21. PMD vs TBD: Kinetic parameters and binding energies for the N-benzylation of 1,2,4-triazole[a,b,c]

energy	X = PMD	X = TBD
$\Delta\Delta^{\ddagger}G$	4.7	4.7
$\Delta\Delta^{\ddagger}G(X)$	10.0	3.2
$\Delta\Delta^{\ddagger}G_1(X)$	19.1	10.8
$\Delta\Delta^{\ddagger}G_4(X)$	4.3	3.0
$\Delta_{Bind}G_{Trz}$	-29	-22
$\Delta_{Bind}G_{Br}$	-12	-13
$\Delta\Delta_{Bind}G(X)$	18	10

[a]All free energies quoted in kJ mol^{-1}. [b]Experimental free energies of activation obtained from classical transition state theory, using the Eyring-Polanyi equation and fitted rate coefficients from kinetic modelling. [c]Experimental rate coefficients for PMD obtained by *in situ* ^{1}H NMR spectroscopy under the following conditions (MeCN-d_3, 20°C): 1,2,4-triazole (50.0 mM), *p*-F-BnBr (50.0 mM), PMD (10.0 – 50.0 mM).

Using these same conditions, the kinetic profiles of *p*-F-BnBr, *p*-F-BnTrz(*N*-1) and *p*-F-BnTrz(*N*-4) were obtained for multiple different loadings of PMD (0.20 – 1.0 equiv., Figure S9) and a global kinetic analysis (Table 2) using the general model in Figure 9. This revealed that the enhanced selectivity achieved with PMD is the combined result of contributions from stronger, more selective triazolate binding [$\Delta_{Bind}G_{Trz}$(PMD) < $\Delta_{Bind}G_{Trz}$(TBD); $\Delta\Delta_{Bind}G$(PMD) > $\Delta\Delta_{Bind}G$(TBD)] and the relative destabilization of the transition state for *N*-1 substitution [$\Delta\Delta^{\ddagger}G$(PMD) > $\Delta\Delta^{\ddagger}G$(TBD)]. These findings are corroborated by DLPNO-CCSD(T) computations (Figures S14-15) and crystallographic studies of the PMDH$^+$Trz$^-$ ion-pair, see later.

11. Phase transfer organocatalysis. With promising selectivity demonstrated in stoichiometric reactions, we set out to develop an *organocatalytic* methodology for the direct *N*-4-alkylation of 1,2,4-triazole. We targeted a strategy based on solid-to-liquid phase transfer catalysis by PMDH$^+$, in which 1,2,4-triazolate anions – derived from a weakly soluble metal triazolate salt (M$^+$Trz$^-$) – are shuttled into solution by a homogeneous organocatalyst, with turnover facilitated by ion-exchange and precipitation of M$^+$X$^-$, Scheme 5. The studies outlined earlier also suggested that halogenated apolar solvents, low temperatures and weakly-coordinating counteranions (X$^-$, Y$^-$) would prove vital. Based on these guiding principles, excellent selectivities and yields were obtained in benylation of potassium 1,2,4-triazolate (K$^+$Trz$^-$) in CH_2Cl_2, by use of catalytic quantities of the tetraphenylborate salt of PMDH$^+$ (Y$^-$ = BPh_4^-).

The reaction is operationally simple, insensitive to air and proceeds to completion within 48 h at 30 °C. Catalyst preparation is trivial and can be conducted on gram-scale from commercially available PMD in one step. Preliminary investigations into reaction conditions, Scheme 5, indicated that increased substrate concentrations increase the rate of product formation, but at the expense of diminished regioselectivity. This arises from two, slow but competitive, processes: a direct *N*-1 selective reaction of the electrophile with the potassium triazolate and a PMDH$^+$-catalyzed *N*-1-alkylation of the product, both leading to reduced selectivity.

Scheme 5. Regioselective phase-transfer organocatalysis[a,b,c,d]

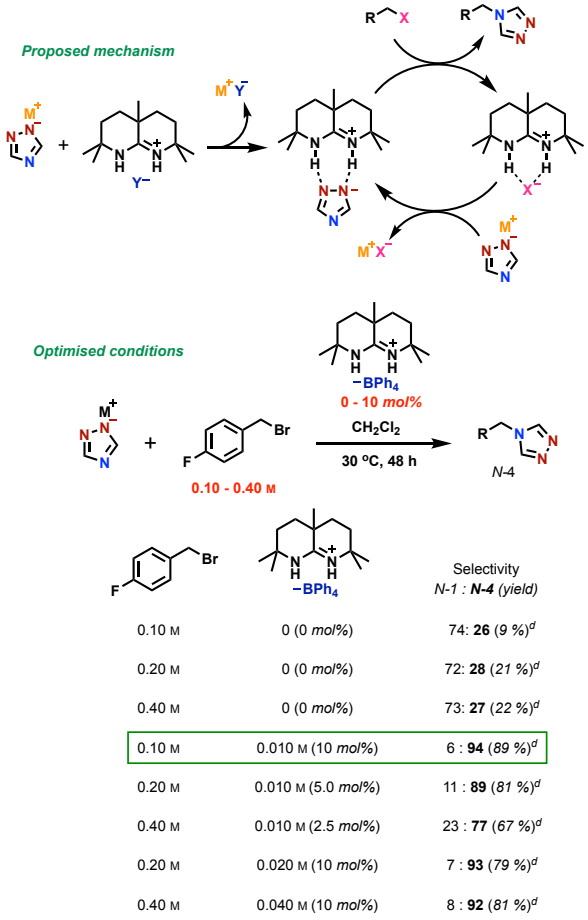

[a]M$^+$Trz$^-$ = Weakly soluble source of 1,2,4-triazolate. [b]Reaction also proceeds with TBDH$^+$BPh$_4^-$ as the catalyst. [c]1.2 equiv. K$^+$Trz$^-$. [d]Yield as estimated by ^{1}H NMR with trimethoxybenzene as internal standard.

Further investigations were conducted with 0.1 M electrophile and 10 mol% catalyst; Scheme 5, to study the effect of the metal countercation M$^+$, the solvent and the catalyst. As expected for a system based on solid-to-liquid phase transfer, a strong correlation between the solubility of the M$^+$Trz$^-$ salt (10 mol%), the polarity of the solvent, and the outcome of the reaction was observed, Scheme 6. As anticipated, $CHCl_3$ proved to be equally as proficient as CH_2Cl_2 in securing high *N*-4 selectivities; non-halogenated apolar solvents of comparable polarity (THF), however, afforded inferior yields of the *N*-4 regioisomer. We next examined the effect of the

metal countercation M^+, the solvent and the catalyst. Polar aprotic (DMSO, Me_2CO, MeCN) solvents reversed the selectivity obtained under optimised conditions, instead favouring *N*-1 substitution (F_{N1} > 50 %).

Scheme 6. Catalytic PMDH$^+$ versus stoichiometric PMD[a,b,c]

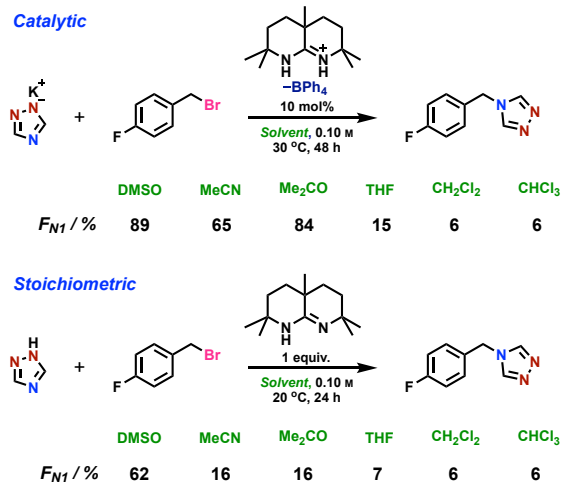

[a]1.2 equiv. K^+Trz^-. [b]Equimolar quantities of 1,2,4-triazole, p-F-BnBr and PMD. [c]F_{N1} = [N_1]/([N_1]+[N_4]). [d]Regioselectivities determined by ^{1}H NMR spectroscopy. [e]F_{N1} = [N_1]/([N_1]+[N_4]).

Compared with stoichiometric conditions, the deterioration in *N*-4 selectivity associated with *non-halogenated* solvents is principally the result higher K^+Trz^- solubility. Indeed, as expected for a system based on solid-to-liquid phase transfer, a strong correlation between the solubility of the M^+Trz^- salt (10 mol%) and the outcome of the reaction was observed. Li^+Trz^- was ineffective (0 % conversion of *p*-F-BnBr, 48 h), Na^+Trz^- gave low conversion (< 25 %, 48 h) but high selectivity. Cs^+Trz^- and K^+Trz^- were equally effective, giving full conversion after 48 h and high *N*-4 selectivity. In stark contrast, $^nBu_4N^+Trz^-$, led to a resurgence in latent *N*-1 selectivity ($F_{N1}(^nBu_4N^+)$ = 85 %), underscoring the importance of controlled, catalyst-mediated phase-transfer.

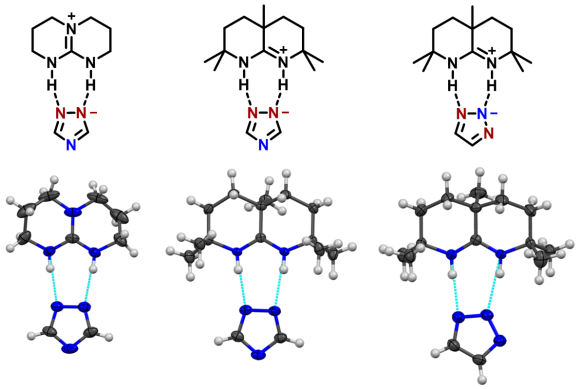

Figure 12. Crystal structures of $TBDH^+Trz^-$, $PMDH^+Trz^-$ and $PMDH^+123Trz^-$, with heavy atoms depicted as ellipsoids at the 70 % probability level. Hydrogen atoms depicted as fixed spheres. Hydrogen-bonded 1,2,3-triazole omitted from crystal structure of $PMDH^+123Trz^-$ for clarity. Crystalline samples prepared by vapor diffusion from CH_2Cl_2/pentanes.

An assortment of organocatalysts were explored to investigate the initiation stage of catalysis (see SI). In the absence of any catalyst only a small proportion of *p*-F-BnBr was consumed after 48 h, leading to trace quantities of the *N*-4 regioisomer (< 5% yield). Compared to $PMDH^+BPh_4^-$, the tetraphenylborate salt of $TBDH^+$ ($TBDH^+BPh_4^-$) was found to be similarly efficient as a *phase-transfer* agent – with *p*-F-BnBr fully consumed after 48 h – but poorer as a non-covalent *protecting group* [$F_{N1}(TBDH^+BPh_4^-)$ = 18 % (*vide supra*). In contrast to $PMDH^+BPh_4^-$ and $TBDH^+BPh_4^-$, classic *neutral* hydrogen bond-donor organocatalysts – including Schreiner's urea and thiourea, and Mattson's urea – afforded only background quantities of the *N*-4 regioisomer (< 5 %), highlighting the importance of *ion-exchange* during initiation.

12. Scope. The optimized methodology was applied to a range of halide-based alkylating agents of varying degrees of reactivity – from unactivated *n*-alkyl iodides through to highly reactive α-bromocarbonyl compounds – furnishing 4-alkyl-1,2,4-triazoles (Scheme 7) with high selectivity (F_{N1} = 87 – 94 %) and good yields (74 – 88 %). In most cases, the extent of deleterious double alkylation was found to be minor. Attempts to effect regioselective *N-4* acylations were not successful.[19,42]

Scheme 7. Regioselective direct alkylation of potassium triazolates catalyzed by PMDH$^+$, compared to alkylations of triazoles mediated by MTBD[a,b,c]

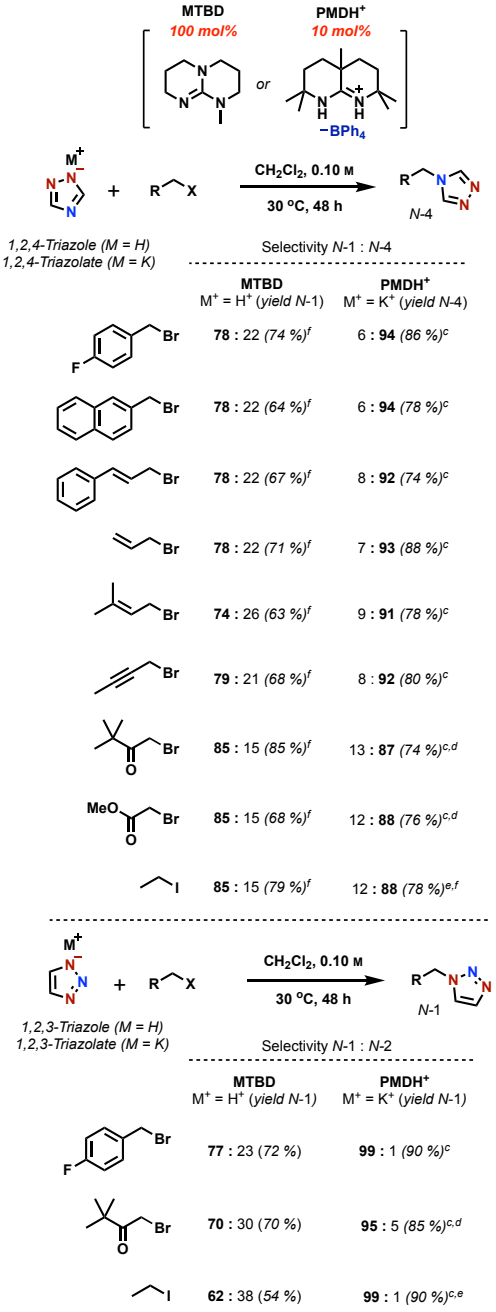

[a]1.2 equiv. K^+Trz^-. [b]Regioselectivities (*N*-1:*N*-4; and *N*-1:*N*-2) determined by ^{1}H NMR spectroscopy. [c]Isolated yields. [d]20 °C. [e]20 mol%, 0.20 M, 40 °C. [f]Yield determined by *in situ* ^{1}H NMR spectroscopy, with 1,3,5-trimethoxybenzene as an internal standard.

The approach also furnishes 1-alkyl-1,2,3-triazoles with high regioselectivity (F_{N1} > 95 %). Indeed, this represents a substantial improvement on selectivities obtained under classic basic conditions, which typically afford significant quantities of both the *N*-1 and *N*-2 alkylated regioisomers (F_{N1} = 67 – 80 %, MTBD; Figure S16). Computational (Figure S16) and crystallographic (Figure 12) studies strongly suggest that the underlying mechanism of regiocontrol is analogous to 1,2,4-triazoles, with regioselective ion-pairing between the $PMDH^+$ cation and 1,2,3-triazolate ($PMDH^+123Trz^-$) selectively protecting the *N*-2 site of the anion.

Comparison of the regioselectivity of MTBD-mediated alkylation of neutral 1,2,4-triazole (*N*-1-selective) with those obtained under $PMDH^+$-catalyzed conditions employing potassium 1,2,4-triazolate (*N*-4-selective), Scheme 7, shows that there is a small increase in *N*-1 selectivity as the electrophilicity of the alkylating agent is increased; with no significant impact of steric effects. Analogous features apply to the reactions of 1,2,3-triazole, and 1,2,3-triazolate.

CONCLUSIONS

Controlling the regioselectivity of ambident triazole nucleophiles towards primary alkylating agents, Scheme 1, has proved challenging for decades[6-17] requiring classic stepwise covalent protection-deprotection and pre-functionalization protocols, Scheme 2, all of which have significant drawbacks.[18-23] Herein, based on detailed mechanistic insight from kinetic, computational, spectroscopic and crystallographic studies, we disclose a regioselective, organocatalytic methodology that bypasses the traditional approach to directly access 4-alkyl-1,2,4-triazoles and 1-alkyl-1,2,3-triazoles in 87-99% regioselectivity, Scheme 7. The operationally simple methodology involves mild conditions (CH_2Cl_2, 30°C, air) and employs reagents and catalysts (K^+Trz^-, $PMDH^+BPh_4^-$) that are trivial to prepare. Many classic halide-based alkylating agents are well tolerated, avoiding the need for prohibitively reactive oxonium and carboxonium species, Scheme 2. In addition, our mechanistic studies reveal that *N*-1 selectivity can be enhanced under the classic basic conditions by employing apolar solvents, and bases that generate weakly-coordinating conjugate acids, Figure 3.

The new approach manipulates the ambident reactivity of the triazolate anions by an *in situ* non-covalent protection strategy in which regioselective ion-pairing between the amidinium cation ($PMDH^+$) and triazolate anions leads to the formation of tightly-bound, but *kinetically competent*, ion-pairs[48] ($PMDH^+Trz^-$) in solution, which we have characterized by KS-DFT/DLPNO-CCSD(T) computations, ^{1}H NMR-DOSY spectroscopy and X-ray crystallography. These ion-pairs retain the reactivity of the liberated anions but exhibit inverted (1,2,4-triazoles) or significantly enhanced (1,2,3-triazoles) regioselectivity towards electrophiles; compare Schemes 1 and 7.

Kinetic analysis and DLPNO-CCSD(T) computations gave substantial insight to the stability and reactivity of the $PMDH^+Trz^-$ ion pair and related species, Figures 6-10. Electrostatic, hydrogen-bonding, and London dispersion interactions, all serve to make complexation between $PMDH^+$ and 1,2,4-triazolate highly exergonic, even in polar aprotic media [K_{Trz}(MeCN) ≈ 180,000]. Moreover, the ability of $PMDH^+$ to serve as a *bidentate* hydrogen-bond donor makes it highly selective towards 1,2,4-triazolate in the presence of diffuse counteranions (Br^-, I^-, BF_4^-, PF_6^-, BPh_4^-). The ion-pairing contribution also renders $PMDH^+$ selective towards 1,2,4-triazolate in the presence of neutral, *N*-alkyl triazoles. Indeed, this dual binding mode is key to preventing catalyst inhibition by product binding under the reaction conditions, Scheme 7. Once 1,2,4-triazolate is bound to $PMDH^+$, the reactivity of the *N*-1 site –the favored site in classic alkylation, Scheme 2 – is suppressed significantly by both charge transfer and hydrogen bonding [$\Delta\Delta^{\ddagger}G_1$(PMD) = 19.1 kJ mol^{-1}, k'_1/k_1 = 2500]. The reactivity of the remote *N*-4 site much less so [k'_4/k_4 = 6]. This *differential* destabilization of the TSs leads to an inversion in the natural regioselectivity of the 1,2,4-triazolate anion towards alkylating agents.

With the newly developed methodology, all but one of the four regioisomers of *N*-alkyl-triazoles can now be obtained in a single alkylation step with high selectivity. More generally, we speculate that application of cationic hydrogen-bond donors such as $TBDH^+$ and $PMDH^+$ need not be confined to the manipulation of triazole anions: many ambident nucleophiles are anionic, and many comprise multiple heteroatoms.[34,43-47]

ASSOCIATED CONTENT

Supporting Information: Additional discussion, experimental procedures, further kinetic data and analysis, computational details, characterization data and NMR spectra. This material is available free of charge via the Internet at http://pubs.acs.org.

AUTHOR INFORMATION

Corresponding Author

guy.lloyd-jones@ed.ac.uk

Notes

The authors declare no competing financial interest.

Funding Sources

The research leading to these results has received funding from the European Research Council under the European Union's Seventh Framework Programme (FP7/2007-2013) / ERC grant agreement n° [340163]). Syngenta and the EPSRC provided an iCASE Award (H.J.A.D.).

ACKNOWLEDGMENT

We thank Andrew Cummins (Edinburgh, UK) for practical assistance in the early phases of this work, Dr Gary Nichol (Edinburgh) for X-ray crystallography, and Professors Jeremy Harvey (Leuven) and Andrew Leach (Liverpool John-Moores) for insightful discussions regarding the computational analyses.

REFERENCES

(1) Breugst, M.; Mayr, H. Ambident Reactivites of Pyridone Anions. *J. Am. Chem. Soc.* **2010**, *132*, 15380–15389.

(2) Hopkins, G. C.; Jonak, J. P.; Tieckelmann, H.; Minnemeyer, H. J. Alkylations of Heterocyclic Ambident Anions. I. 2-Hydroxypyrimidines. *J. Org. Chem.* **1966**, *31*, 3969–3973.

(3) Hopkins, G. C.; Jonak, J. P.; Minnemeyer, H. J.; Tieckelmann, H. Alkylations of Heterocyclic Ambident Anions II. Alkylation of 2-Pyridone Salts. *J. Org. Chem.* **1967**, *32*, 4040–4044.

(4) Haque, M. R.; Rasmussen, M. Ambident Heterocyclic Reactivity: Alkylation of 2-Substituted-4-Methylbenzimidazoles. *Tetrahedron* **1994**, *50*, 5535–5554.

(5) Mahadevan, I.; Rasmussen, M. Ambident Heterocyclic Reactivity: The Alkylation of Pyrrolopyridines (Azaindoles, Diazaindenes). *Tetrahedron* **1993**, *49*, 7337–7352.

(6) Claramunt, R. M.; Elguero, J.; Garceran, R. Synthesis of Azoles by PTC. *Heterocycles* **1985**, *23*, 2895

(7) Atkinson, M. R.; Polya, J. B. Part II. N-Substitution of Some 1,2,4-Triazoles. *J. Chem. Soc.* **1954**, *0*, 141.

(8) Märky, M.; Schmid, H.; Hansen, H. J. Photoreaktionen von 1-Alkylbenztriazolen. *Helv. Chim. Acta* **1979**, *62*, 2129–2153.

(9) Potts, K. T. The Chemistry of 1,2,4-Triazoles. *Chem. Rev.* **1961**, *61*, 87–127.

(10) Holm, S. C.; Straub, B. F. Synthesis of *N* -Substituted 1,2,4-Triazoles. A Review. *Org. Prep. Proced. Int.* **2011**, *43*, 319–347.

(11) Bulger, P. G.; Cottrell, I. F.; Cowden, C. J.; Davies, A. J.; Dolling, U. An Investigation into the Alkylation of 1 , 2 , 4-Triazole. *Tetrahedron Lett.* **2000**, *41*, 1297–1301.

(12) Katritzky, A. R.; Wojciech, K.; Greenhill, J. V. An Improved Method for the N-Alkylation of Benzotriazole and 1,2,4-Triazole. *Recl. des Trav. Chim. des Pays-Bas.* **1991**, *110*, 369.

(13) Ohta, S.; Kawasaki, I.; Uemura, T.; Yamashita, M.; Yoshioka, T.; Yamaguchi, S. Alkylation and Acylation of the 1,2,3-Triazole Ring. *Chem. Pharm. Bull.* **1997**, *45*, 1140–1145.

(14) Wang, X.; Zhang, L.; Krishnamurthy, D.; Senanayake, C. H.; Wipf, P. General Solution to the Synthesis of N -2-Substituted 1 , 2 , 3-Triazoles. *Org. Lett.* **2010**, *12*, 4632.

(15) Huxley, M. T.; Burgun, A.; Ghodrati, H.; Coghlan, C. J.; Lemieux, A.; Champness, N. R.; Huang, D. M.; Doonan, C. J.; Sumby, C. J. Protecting-Group-Free Site-Selective Reactions in a Metal-Organic Framework Reaction Vessel. *J. Am. Chem. Soc.* **2018**, *140*, 6416–6425.

(16) Koren, A. O. Acid-Mediated Regioselective Alkylation of 1,2,3-Triazole. *J. Heterocycl. Chem.* **2002**, *39*, 1111.

(17) Begtrup, M.; Larsen, P. Alkylation, Acylation and Silylation of Azoles. *Acta Chemica Scandinavica*. **1990**, 44, 1050–1057.

(18) Olofson, R. A.; Kendall, R. V. Protection by Acylation in the Selective Alkylation of Heterocycles. *J. Org. Chem.* **1970**, *35*, 2246–2248.

(19) Astleford, B. A.; Goe, G. L.; Keay, J. G.; Scriven, E. F. V. Synthesis of 1-Alkyl-1,2,4-Triazoles: A New One-Pot Regiospecific Procedure. *J. Org. Chem.* **1989**, *54*, 731–732.

(20) Rostovtsev, V. V; Green, L. G.; Fokin, V. V; Barry Sharpless, K. A Stepwise Huisgen Cycloaddition Process: Copper(I)-Catalyzed Regioselective "Ligation" of Azides and Terminal Alkynes. *Angew. Chem. Int. Ed.,* **2002**, *41*, 2596.

(21) Tornøe, C. W.; Christensen, C.; Meldal, M. Peptidotriazoles on Solid Phase: [1,2,3]-Triazoles by Regiospecific copper(I)-Catalyzed 1,3-Dipolar Cycloadditions of Terminal Alkynes to Azides. *J. Org. Chem.* **2002**, *67*, 3057–3064.

(22) Zhang, L.; Chen, X.; Xue, P.; Sun, H. H. Y.; Williams, I. D.; Sharpless, K. B.; Fokin, V. V.; Jia, G. Ruthenium-Catalyzed Cycloaddition of Alkynes and Organic Azides. *J. Am. Chem. Soc.* **2005**, *127*, 15998–15999.

(23) Boren, B. C.; Narayan, S.; Rasmussen, L. K.; Zhang, L.; Zhao, H.; Lin, Z.; Jia, G.; Fokin, V. V. Ruthenium-Catalyzed Azide− Alkyne Cycloaddition: Scope and Mechanism. *J. Am. Chem. Soc.* **2008**, *130*, 8923–8930.

(24) Wiskur, S. L.; Lavigne, J. J.; Metzger, A.; Tobey, S. L.; Lynch, V.; Anslyn, E. V. Thermodynamic Analysis of Receptors Based on Guanidinium/boronic Acid Groups for the Complexation of Carboxylates, α-Hydroxycarboxylates, and Diols: Driving Force for Binding and Cooperativity. *Chem. Eur. J.* **2004**, *10*, 3792–3804.

(25) Houk, R. J. T.; Tobey, S. L.; Anslyn, E. V. Abiotic Guanidinium Receptors for Anion Molecular Recognition and Sensing. *Top. Curr. Chem.* **2005**, *255*, 199–229.

(26) Linton, B. R.; Scott Goodman, M.; Fan, E.; Van Arman, S. A.; Hamilton, A. D. Thermodynamic Aspects of Dicarboxylate Recognition by Simple Artificial Receptors. *J. Org. Chem.* **2001**, *66*, 7313–7319.

(27) Haj-Zaroubi, M.; Mitzel, N. W.; Schmidtchen, F. P. The Rational Design of Anion Host Compounds: An Exercise in Subtle Energetics. *Angew. Chem. Int. Ed.* **2002**, *41*, 104–107.

(28) Berger, M.; Schmidtchen, F. P. The Binding of Sulfate Anions by Guanidinium Receptors Is Entropy-Driven. *Angew. Chem. Int. Ed.* **1998**, *37*, 2694–2696.

(29) Blondeau, P.; Segura, M.; Pérez-Fernández, R.; de Mendoza, J. Molecular Recognition of Oxoanions Based on Guanidinium Receptors. *Chem. Soc. Rev.* **2007**, *36*, 198–210.

(30) Fu, X.; Loh, W. T.; Zhang, Y.; Chen, T.; Ting, M.; Liu, H.; Wang, J.; Tan, C. H. Chiral Guanidinium Salt Catalyzed Enantioselective Phospha-Mannich Reactions. *Angew. Chem. Int. Ed.* **2009**, *48*, 7387–7390.

(31) Dong, S.; Liu, X.; Zhu, Y.; He, P.; Lin, L.; Feng, X. Organocatalytic Oxyamination of Azlactones: Kinetic Resolution of Oxaziridines and Asymmetric Synthesis of Oxazolin-4-Ones. *J. Am. Chem. Soc.* **2013**, *135*, 10026–10029.

(32) Uyeda, C.; Jacobsen, E. N. Transition-State Charge Stabilization through Multiple Non-Covalent Interactions in the Guanidinium-Catalyzed Enantioselective Claisen Rearrangement. *J. Am. Chem. Soc.* **2011**, *133*, 5062–5075.

(33) Dong, S.; Feng, X.; Liu, X. Chiral Guanidines and Their Derivatives in Asymmetric Synthesis. *Chem. Soc. Rev.* **2018**, *47*, 8525–8540.

(34) Mayr, H.; Breugst, M.; Ofial, A. R. Farewell to the HSAB Treatment of Ambident Reactivity. *Angew. Chem. Int. Ed.* **2011**, *50*, 6470–6505.

(35) Breugst, M.; Zipse, H.; Guthrie, J. P.; Mayr, H. Marcus Analysis of Ambident Reactivity. *Angew. Chem. Int. Ed.* **2010**, *49*, 5165.

(36) Reichardt, C. Solvatochromic Dyes as Solvent Polarity Indicators. *Chem. Rev.* **1994**, *94*, 2319–2358.

(37) Reichardt, C. Empirical Parameters of the Polarity of Solvents. *Angew. Chem. Int. Ed.* **1965**, *4*, 29–40.

(38) Kamlet, M. J.; Abboud, J. L. M.; Abraham, M. H.; Taft, R. W. Linear Solvation Energy Relationships. 23. A Comprehensive Collection of the Solvatochromic Parameters, Π, A, and B, and Some Methods for Simplifying the Generalized Solvatochromic Equation. *J. Org. Chem.* **1983**, *48*, 2877–2887.

(39) Taylor, J. E.; Bull, S. D.; Williams, J. M. J. Amidines, Isothioureas, and Guanidines as Nucleophilic Catalysts. *Chem. Soc. Rev.* **2012**, *41*, 2109.

(40) Dworniczak, M.; Leffek, K. T. Proton transfer reactions between 4-nitrophenylphenylcyanomethanes and cyclic nitrogen bases in acetonitrile. *Can. J. Chem.* **1990**, *68*, 1657.

(41) Raab, V.; Gauchenova, E.; Merkoulov, A.; Harms, K.; Sundermeyer, J.; Kovačević, B.; Maksić, Z. B. 1,8-Bis(hexamethyltriaminophosphazenyl)naphthalene, HMPN: A Superbasic Bisphosphazene "proton Sponge." *J. Am. Chem. Soc.* **2005**, *127*, 15738–15743.

(42) Yang, X.; Birman, V. B. Acyl Transfer Catalysis with 1,2,4-Triazole Anion. *Org. Lett.* **2009**, *11*, 1499–1502.

(43) Tishkov, A. A.; Schmidhammer, U.; Roth, S.; Riedle, E.; Mayr, H. Ambident Reactivity of the Nitrite Ion Revisited.

Angew. Chem. Int. Ed. **2005**, *44*, 4623–4626.

(44) Schaller, H. F.; Schmidhammer, U.; Riedle, E.; Mayr, H. Ambident Reactivity of the Cyanate Anion. *European J. Org. Chem.* **2008**, *14*, 3866–3868.

(45) Tishkov, A. A.; Mayr, H. Ambident Reactivity of the Cyanide Ion: A Failure of the HSAB Principle. *Angew. Chem. Int. Ed.* **2005**, *44*, 142–145.

(46) Loos, R.; Kobayashi, S.; Mayr, H. Ambident Reactivity of the Thiocyanate Anion Revisited : Can the Product Ratio Be Explained by the Hard Soft Acid Base Principle ? *J. Am. Chem. Soc.* **2003**, *125*, 14126–14132.

(47) Dong, H.; Rahm, M.; Thota, N.; Deng, L.; Brinck, T.; Ramström, O. Control of the Ambident Reactivity of the Nitrite Ion. *Org. Biomol. Chem.* **2013**, *11*, 648–653.

(48) The analogous effect is operative in the urea-fluoride H-bonded nucleophilic anions pioneered by Gouverneur: see: Pupo, G.; Chiara Vicini, A. C.; Ascough, D. M. H.; Ibba, F.; Christensen, K. E.; Thompson, A.L.; Brown, J. M.; Paton, R. S.; Gouverneur, V. *J. Am. Chem. Soc*., **2019**, *141*, 2878–2883, and references therein.

GRAPHICAL ABSTRACT